Development of an Indoor Line Scanning System for Photovoltaic Modules Performance Characterization

Moses Oboo [a*], Denis Okello [a], Willy Okullo [a] and Bosco Oryema [b]

[a] Department of Physics, College of Natural Sciences, Makerere University P. O. Box:7062, Kampala City, Uganda.
[b] Department of Physics, Muni University, P. O. Box: 725, Arua City, Uganda.

Authors' contributions

Original Research Article

ABSTRACT

Uganda's interest in using solar energy for various applications began 20 years ago. However, there have been numerous reports by the public over the poor performance of the photovoltaic (PV) modules during their operations. This study determined the performance of selected PV modules openly sold in the Ugandan markets. The low-cost indoor line scanning system developed using locally available materials was used to assess the performance of each of the solar cells in the PV module by determining their photogenerated currents. In addition, the electrical characteristics of the PV modules were determined using the outdoor characterization method, which assumed the actual operation of the PV modules under direct sunlight. From the indoor line scans, the

_____

Corresponding author: E-mail: mosesoboo@gmail.com;

percentage of performing solar cells in the three PV modules of single-crystalline silicon (c-Si), multi-crystalline silicon (mc-Si), and amorphous silicon (a-Si) technologies were determined as 79%, 61%, and 95% respectively. The outdoor characterization results revealed that the c-Si, mc-Si, and a-Si PV modules had measured maximum power outputs of 18.5 W, 19.0 W, and 18.9 W, respectively and these were lower than the rated power values of 20 W. The line scan results had a direct relationship with the measured power output of the PV module, which implied that solar cells mismatch, affected the performance of the PV modules by lowering their performance. This developed testing system is affordable for developing countries with limited testing systems and would in the long run contribute to significant increase in the deployment of PV technology in Uganda since only performing PV modules would be allowed into the open market.

NOMENCLATURE

PV   : *Photovoltaic*
a-Si   : *Amorphous Silicon*
c-Si   : *Single Crystalline Silicon*
DAQ   : *Data Acquisition*
LCOE : *Levelized Cost of Electricity*
m-Sci : *Multi-Crystalline Silicon*
MW   : *Mega Watts*
STC   : *Standard Test Conditions*
θ : *Zenith Angle*
V_n : *Normalized Voltage*
V_m : *Measured Voltage*

1. INTRODUCTION

The energy resources in every nation play vital roles in its social and economic transformation since they are applied in domestic, industrial, and technological sectors (Zhang et al., 2019). In Uganda, there is an enormous demand for energy, arising from the increasing industrialization and high population of approximately 44.2 million people coupled with the rapid population growth rate of 3.3% per annum (Fashina et al., 2018). The country's energy sector is not sufficient enough to handle the increasing energy demands (Aarakit, Ssennono, et al., 2021). At present, Uganda's total installed energy generation capacity is 2,048.1 MW, with hydropower accounting for 84%, bagasse co-generation at 7%, thermal electricity at 5%, and solar photovoltaics at 4% (Electricity Regulatory Authority, 2024). Solar energy although having the lowest capacity still remains as the best renewable energy source in the world (Lee & Chang, 2018).

According to Uganda Vision 2040, the estimated energy production will be 52.5 GW in 2040, with solar PV technologies projected to provide 5,000 MW (Micheal et al., 2018). The solar energy technology is the cheapest and most sustainable renewable energy source that provides clean energy and contributes greatly in the reduction of ecological problems globally, particularly CO_2 emissions (Al-Dousari et al., 2019; Gebreslassie, 2021; Islam et al., 2018; Kumar & Kumar, 2019). Globally, solar energy is projected to contribute 60% of the total capacity by 2025 (Rabelo et al., 2021). This projection is quite feasible as long as reliability, accessibility, and performance issues are routinely monitored and rectified. The amount of solar photovoltaic (PV) modules installed on residential rooftops and utility rooftops has increased dramatically in recent years. Long-term warranties, scalability, affordability, and the steady decline in the levelized cost of electricity (LCOE) for solar PVs across the globe are all major contributors to this trend (Celik et al., 2017; da Fonseca et al., 2020; Sun et al., 2017).

In the past 20 years, Uganda has witnessed increased demand for solar energy, especially in areas not connected to the national grid. The increase is attributed to the availability of PV modules at local markets, and their affordability (Aarakit, Ntayi, et al., 2021). Due to the country's geographical location along the equator, it has an abundance of sunlight with an hourly direct normal solar radiation intensity of 500 Wm^{-2}, expected between 09:00 hours and 16:00 hours in most parts of the country (Okello et al., 2011). This makes solar energy more favorable for use in most parts of the country. Currently, Uganda imports PV modules from the US, Germany, India, China, and the UK. These modules are being extensively used domestically on small scales in both rural and urban areas for lighting purposes in schools, homes, town streets, hospitals, etc., and for powering devices like fridges, charging mobile phones, and other electronic devices (van Hove & Johnson, 2021).

The industrial implementation of photovoltaic (PV) modules in Uganda is a growing sector driven by the need for reliable and sustainable energy solutions. This expansion is primarily motivated by the need to increase energy access, and reduce on use of biomass fuels (Mugagga et al., 2019).

Uganda has made strides in the solar energy sector with notable plants like the MSS Xsabo Solar Power Limited generating 10 MW while both Soroti and Tororo Solar Power Stations produce 10 MW (Avellino et al., 2018; (Mugagga et al., 2019). These facilities are key to Uganda's efforts in expanding its renewable energy sources. Furthermore, the government initiatives such as tax exemptions on solar products and partnerships with international donors for rural electrification projects, have significantly spurred growth in this sector (Fashina et al., 2018).

As much as Uganda is increasingly embracing solar technology, there is a growing outcry by the public on the poor performance of PV modules, which operate for a shorter period. The poor performance of the PV modules could be attributed to cell mismatch during manufacturing (Alonso-Garcia et al., 2006; Kaushika & Rai, 2007), damage to the solar cells during transportation (Tyagi et al., 2013), poor storage of the solar modules at the factories or selling centers (Luo et al., 2021), dust concentration on the solar modules (Santhakumari & Sagar, 2019; Shenouda et al., 2022; Singh et al., 2022), humidity (Hasan et al., 2022; Kazem & Chaichan, 2015; Touati et al., 2013), temperature, wind speed (Tahir et al., 2022), and poor system pre-installation (Akinyele et al., 2015). Many factors affect the performance of PV modules, and this study specifically focused on investigating the performance levels of PV modules openly sold in Ugandan markets to ascertain if they have standardized performance.

There have been some related studies on assessment of the performance of the PV modules in the world. This research was arrived at after careful review of the related studies in some African countries, where solar cell mismatch before installation was identified as one of the major challenges affecting the PV technology performance. Table 1 gives some of the similar researches conducted in other African countries.

In this study, the indoor line scanning technique was used to carefully scan each solar cell to determine their photogenerated currents when illuminated. In addition, an outdoor characterization method was used to evaluate the performance of the same PV modules when installed on the rooftop of a buiding. The goal was to compare the measured electrical properties of the PV module to the specifications listed on the PV module's nameplate.

2. METHODS AND MATERIALS

2.1 PV Modules Used in the Study

This study used three PV modules of a 20 Wp power rating from the same manufacturer with different technologies of c-Si, mc-Si, and a-Si types as shown in Fig. 1. Table 2 shows the specifications of the PV modules used in this study. The c-Si, mc-Si, and a-Si PV modules had 48, 56, and 20 solar cells respectively. A smaller number of PV modules with a low power rating were used to reduce the cost of purchasing PV modules from the open market since wattage is directly proportional to the price of the PV module.

Fig. 1. The PV modules of different technologies used in this study

Table 1. Comparison of the our research with PV experience in other African countries

Research topic and country	Research findings and References
Solar photovoltaic modules' performance reliability and degradation analysis study conducted in Ethiopia	The study highlights the effectiveness of various assessment techniques, including electroluminescence and thermography, and recommends integrating advanced machine learning models for predictive maintenance and improved performance assessment. The research underscores the importance of early defect detection and data-driven approaches to enhance PV module reliability and longevity in Ethiopia (Alimi et al., 2022)
Thermal Infrared and Visual Inspection of Photovoltaic Installations by UAV Photogrammetry—Application Case: Morocco	Using thermal and visual imagery taken by unmanned aerial vehicles (UAVs), this study inspected photovoltaic installations, detecting visual defects such as cracks, soiling, and hotspots, and developed a semi-automatic procedure for hotspots' extraction, demonstrating the potential of UAV imagery for effective PV system inspections. (Zefri et al., 2018).
The study on the effect of technological mismatch on photovoltaic array: Analysis of Relative Power Loss : Case study in Nigeria	The study developed an equivalent circuit model to analyze maximum Fill Factor (FF) and Relative Power Losses (RPL) for different module configurations. The results showed that matched modules had negligible RPL, while mismatched modules exhibited RPL of 1.3% in Parallel (P) and Series-Parallel (SP) configurations and 2.6% in Series (S) configuration, suggesting the use of SP configuration and uniform modules to minimize RPL in large photovoltaic plants. (Nnamchi et al., 2021) .
Investigation and analysis of defects and degradations in desert fielded photovoltaic modules in Algeria	The study of five-year-old PV modules in Dubai's desert environment identified significant defects such as structural breakages, glass abrasions, and encapsulant discoloration, highlighting the need for new standard tests tailored to desert conditions due to these defects not being detected under existing protocols.(S. Kumar et al., 2021)
Investigation into the impacts of design, installation, operation and maintenance issues on performance and degradation of installed solar PV systems in Ghana	Design and Installation Issues: The study found that many installers ignored proper PV system design procedures, resulting in systems that were undersized and unable to meet the energy demands agreed upon with the owners. Overall, 69% of the systems were improperly sized, which led to lower than expected power output and system failures. (Aboagye et al., 2022).
Photovoltaic module quality in the Kenyan solar home systems market	There was a significant variability in the quality of PV modules available in the market. While many brands offer high quality and reliable products. There are also numerous substandard modules that failed to meet expected performance standards.(Duke et al., 2002)
Identification and characterization of performance limiting defects and cell mismatch in photovoltaic modules in South Africa	The degraded modules exhibited current mismatch, as evidenced by the I-V curves and supported by the Electroluminescence (EL) images. The study demonstrated that combining EL imaging with I-V curve analysis effectively characterizes the degradation in PV modules, highlighting the importance of identifying and addressing cell mismatch to maintain PV module performance and longevity (Crozier et al., 2015)
Correlation of Infrared Thermal Imaging Results	The results showed that the higher the temperature difference in the hot spot tests, the higher the rate

Research topic and country	Research findings and References
with Visual Inspection and Current-Voltage Data of PV Modules Installed in Kumasi, a Hot, Humid Region of Sub-Saharan Africa of Ghana	of power degradation. 11 out of the 14 PV modules assessed failed the hot spot tests. The power performance factor for all 14 modules fell below the average 80% standard set by most manufacturers for modules operating within the 25-year warranty. (Takyi, 2017).
Fault identification of photovoltaic array based on machine learning classifiers study conducted in Egypt	This study developed an optimal machine learning (ML) algorithm for detecting and diagnosing common photovoltaic (PV) array faults, including permanent faults (Arc Fault, Line-to-Line, Maximum Power Point Tracking unit failure, and Open-Circuit faults) and temporary faults (Shading). The researchers compared Decision Tree (DT), K-Nearest Neighbors (KNN), and Support Vector Machine (SVM) classifiers, using different splitting criteria, distance metrics, weighting functions, and kernel functions. Both simulation and experimental case studies demonstrated that the SVM classifier, optimized with Bayesian methods, provided the best performance in accurately identifying and diagnosing PV array faults under diverse conditions. (Badr et al., 2021).

Table 2. Specifications of the PV modules

Parameters	c-Si	mc-Si	a-Si
Rated maximum power P_{max} (Wp)	20.0	20.0	20.0
Current at P_{max} (A)	1.15	1.11	1.11
Voltage at P_{max} (V)	17.6	18.0	18.0
Short circuit current (A)	1.27	1.24	1.2
Open circuit voltage (V)	21.4	21.6	29.0
Efficiency (%)	16.2	8.80	5.10
PV module area (m²)	0.125	0.227	0.394
Number of solar cells	48	56	20

2.2 The Indoor Line Scanning System

2.2.1 Design of the system

The materials used to fabricate the system included a car wiper motor, pulleys, a laser diode, a laser diode holding system, wire rope, and metallic hollow sections as shown in Fig. 2. The fabrication was conducted such that the developed system accommodates the surface area of each selected PV module. The key instruments used to achieve the research objectives of this study are listed in Table 3.

2.2.2 Choice of the laser diode for the study

The wavelength of 635 nm was selected for the diode because at this wavelength, the surface reflectance is 0% and the internal and external quantum efficiencies of the photovoltaic modules are 100% (Devi et al., 2021). The laser diode beam had a spot diameter of 1.5 mm thus the beam area was $1.768 \times 10^{-6} \ m^2$ with beam intensity of $2.828 \times 10^6 \ Wm^{-2}$ (Kaspari et al., 2008). Fig. 3 illustrates how these factors change at different spectrum wavelengths.
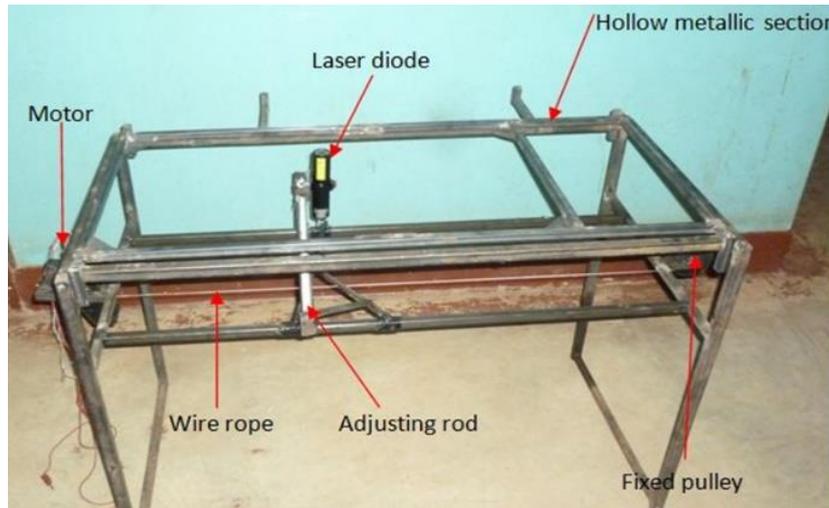

Fig. 2. The fabricated frame of the indoor line scanning system

Table 3. Instruments and their purpose in the research study

| Name of the instrument	Purpose
Laser diode	Provided the only source of light for scanning the PV modules
Motor	Provide mechanical energy to run the laser diode across the solar cells
Pre-Amplifier	Increase the photogenerated currents to measurable values
Spirit level	Ensuring the PV modules are placed normally to the roof surface
Computer	For running the LabView and MATLAB soft wares
Variable resistor	Varying the resistance during outdoor characterization measurements
Multimeter	Measure the module and ambient temperatures
Tape measure	Measuring the dimensions of the PV modules
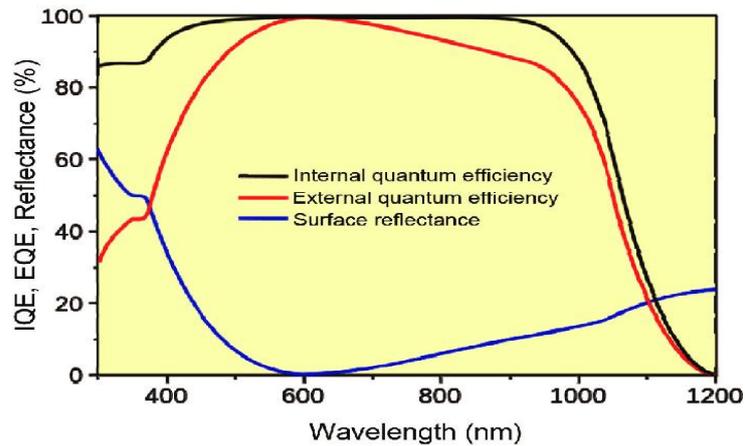
Fig. 3. Variation of surface reflectance, internal and external quantum efficiency with wavelength of a photovoltaic module

2.2.3 The line scanning of the PV modules

Fig. 4 shows the experimental setup placed in a dark room to avoid illuminations from other sources of light. This ensured that only light from the laser diode (wavelength 635 nm) was incident on the selected PV module. The chosen PV module was put in a rack so that the metallic contacts were parallel to the scanning direction. The system was set into motion by turning on the motor, which spun the pulley and made the laser diode move at the speed of the motor. The speed of the motor during the scanning process was set by adjusting the voltage and all the PV modules were scanned at the same speed of motion of the laser diode. A pulley was fixed onto the motor and the wire rope was made to pass over the pulley and connect to the other pulley via a system holding the laser diode. In the system, the movement of the motor is transmitted to the pulley, which in turn moves the laser diode system connected to the wire rope.

The pre-amplifier connected to the PV module amplified the small-generated currents in pico-amperes to measurable values and delivered them to the Data Acquisition (DAQ) system and to the computer, where readings and line scans were displayed.

The computer connected to the PV module had an installed LabView program that started running as soon as the beam from the laser diode touched the PV module and line scans of the outputs of the photo-generated currents of each solar cell were displayed on the computer. After completing the scanning of the first string, the reverse scanning of the next string was conducted after adjusting the laser diode. This process was repeated until all the solar cells in all the strings of the PV module were scanned. The photogenerated currents for all the solar cells were then merged and plotted to obtain the line scans of the whole PV module. This procedure was repeated for all three types of the selected PV modules.
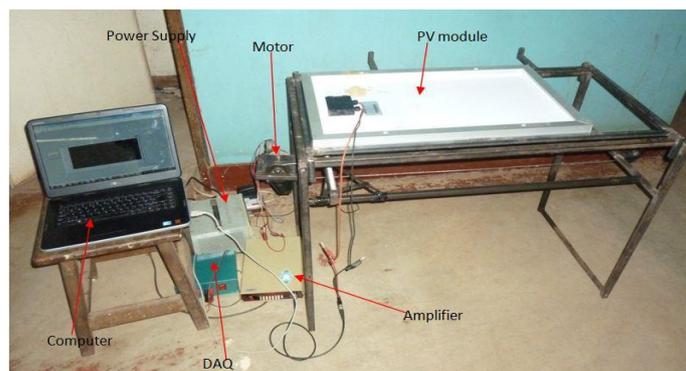

Fig. 4. Experimental setup for the indoor line scanning system

2.2.4 Determining the proportion of performing solar cells

To determine the proportion of performing solar cells, all the solar cells whose photogenerated currents were nearly equal to zero were considered non-performing solar cells (almost dead solar cells), and the rest were considered performing solar cells. The percentage of the performing solar cells was computed using the equation

$$P_s = \frac{100A}{T} \% \tag{1}$$

where A is the number of performing solar cells, T is the total number of solar cells in the PV module, and P_s is the percentage of performing solar cells.

2.2.5 Outdoor characterization of the PV modules

During outdoor characterization, each PV modules was exposed to solar irradiance at a zenith angle of zero degrees since this position ensured normal incidence at the time of the experiment (Yunus Khan et al., 2020). This was achieved by conducting the experiment at solar noon on a flat roof top surface that allowed for the PV module to operate optimally such that at this inclination the PV module would produce the maximum photogenerated current according to the equation.

$$I_{ph} = I_{max}\cos\theta \tag{2}$$

where I_{ph} is the photogenerated current, I_{max} is the maximum current generated and   is the zenith angle.

The solar radiation was measured using the Apogee Instruments SP-510 pyranometer that is known for its accuracy, stability, durability, and cost-effectiveness (Blonquist Jr & Bugbee, 2020). The variable resistor as a load method was used to characterize the PV modules. Fig. 5 shows the experimental setup for outdoor characterization on the open rooftop.

For easy and convenient measurements of variables, a DAQ card was integrated into the system and the circuit is shown in Fig. 6.

The DAQ card used has a voltage range of $0 - 5$ V and this is why a potential divider consisting of resistances R_1 and R_2 were incorporated into the system. The value of the shunt resistance of 0.0075 Ω is considered to be insignificant in comparison to the values of R_1 and R_2 and hence it is not considered part of the potential divider. The DAQ measures the voltage across R_2 according to the equation 3.

$$V_{R_2} = \left(\frac{R_2}{R_1 + R_2}\right)V_P = \left(\frac{20}{20 + 100}\right)V_P = \frac{V_P}{6} \tag{3}$$

where V_P is the voltage across the PV module.

The DAQ measures the voltage across the shunt and when this voltage is divided by the shunt resistance as shown in the block diagram in Fig. 5, it configures the DAQ to measure the current through the shunt which is the current generated by the PV module as shown in equation 4.

$$I_P = I_{shunt} = \frac{V_{shunt}}{R_{shunt}} \tag{4}$$

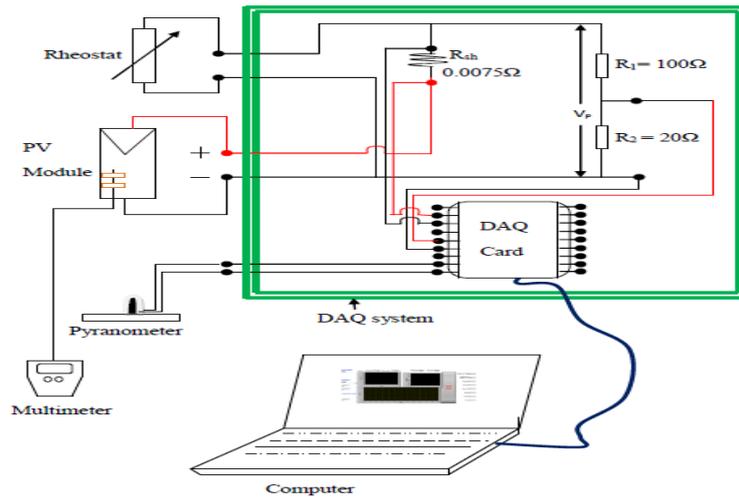**Fig. 5. Experimental setup for outdoor characterization**

Fig. 6. A detailed diagram of a variable resistor as a load method for I-V characterization

The short-circuit current I_{sc} was obtained when the resistance of the rheostat was zero and the open circuit voltage V_{OC} was obtained when the resistance of the rheostat was maximum. The other parameter measured by the DAQ is the solar irradiance. Module and ambient temperatures were measured using a multimeter. To measure module temperature the cable from the thermocouple attached at the back of the module was plugged into the multimeter.

The I-V Tracing program designed in LabView was used to trace the I-V characteristics of the PV modules. The program was set to run co-currently with the sliding contact on the rheostat varying from minimum to maximum resistance. For each complete run of the program, both the I-V and the solar cell electrical parameters of open circuit voltage (V_{OC}), short-circuit current (I_{sc}), maximum power (P_{max}), maximum voltage (V_{max}), maximum current (I_{max}) and the fill factor (FF) were saved on the computer automatically. When the sliding contact is at the position of zero resistance, the current value is maximum and equals I_{sc} and the voltage value equals zero.

On the other hand, when the sliding contact is at the maximum resistance of the rheostat, the current drops to zero and the voltage value attained is V_{OC}. This was conducted five times a day between 10:00 hours and 15:00 hours when the solar radiation was at least 800 Wm⁻². After the normalization of the I-V data, the plot of current against voltage gave the I-V characteristics of each PV module (Cáceres et al., 2020).

The saved I-V data were normalized to Standard Test Conditions (STCs) before it was run in a program designed in Matlab to obtain the desired electrical parameters of the PV module (Padilla et al., 2022). The STCs are industry standard conditions under which solar PV modules are tested to determine their rated power and other electrical characteristics (De la Parra et al., 2017; Hejri & Mokhtari, 2016; Ibrahim & Anani, 2017).

For the I–V data normalization, a modified version of IEC 60891:2021 (Procedures for temperature and irradiance corrections to measure I–V characteristics) was applied (Li et al., 2023; Quansah et al., 2017). The solar module measured current was normalized using equation 5

$$I_2 = I_1(1 + \alpha(T_2 - T_1) \times \frac{G_2}{G_1} \quad (5)$$

where I_2 is the normalized current (A), I_1 is the measured current (A), G is solar irradiance (Wm⁻²), T is module temperature (ºC), and α is the temperature coefficient for current. Subscripts 1 and 2 refer to the measured values, and values at reference conditions respectively. Similarly, the module voltage was normalized using equation 6 given by (Chamberlin et al., 1995)

$$Vn = V_m\{1 + b(T - 25ºC)\} \quad (6)$$

where V_n is the normalized voltage in volts, V_m is the measured voltage in volts, *b* is the temperature coefficient per degree Celsius,

and T is the module temperature in degrees Celsius.

The efficiency for each PV module was calculated using the measured electrical parameters according to the equation

$$\eta_{max} = \frac{P_{max}}{P_{in}} \times 100 = \frac{V_{max} \times I_{max}}{E \times A} \times 100 \qquad (7)$$

where E is the irradiance or total incident power per square meter and A is the total area of the solar cells.

The calculated efficiency values were then compared with the manufacturer's rated values on the PV modules. The results of the measurements and calculations are discussed in the following section.

3. RESULTS AND DISCUSSION

3.1 Indoor Line Scans

The scanning of the PV modules was conducted by following each string, which in PV technology is defined as a series of solar cells or PV modules that are electrically connected in series to form a larger array (Huld et al., 2010). A line scan of the entire PV module was created by combining the results of the individual scans of each string. The results of the line scans are in Figs 7-9.

The line scans of each PV module show that the solar cells have different performance levels, leading to a solar cell mismatch that affects the overall PV module performance. Some of the solar cells produced very low currents after being struck by photons and were nearly regarded as dead solar cells. The current mismatches between the worst performing and best performing solar cells in c-Si, mc-Si and a-Si were 99.9%, 97.4% and 79.2% respectively. The current mismatch of the solar cells in a PV module is a phenomenon that occurs when the solar cells have different electrical characteristics (Wurster & Schubert, 2014). This can lead to reduced power output and efficiency of the module, as well as potential damage to the cells due to overheating or reverse biasing (Crozier et al., 2012).

In this research study, the environmental causes of solar cell current mismatch like shading, and dust accumulation were controlled during the experimental work. Therefore, the most likely causes of current mismatch between the solar cells was during the solar module manufacturing processes like a lack of solar cell sorting, and slight differences in the solar cells material properties, such as doping concentration, thickness, or defect density, which can affect their electrical parameters (Bakas et al., 2012). Another factor is spectral mismatch where the solar cells may have different spectral responses to the incident light, depending on their band gap, absorption coefficient, or anti-reflective coating resulting in different current generation under different illumination conditions (Chantana et al., 2019).
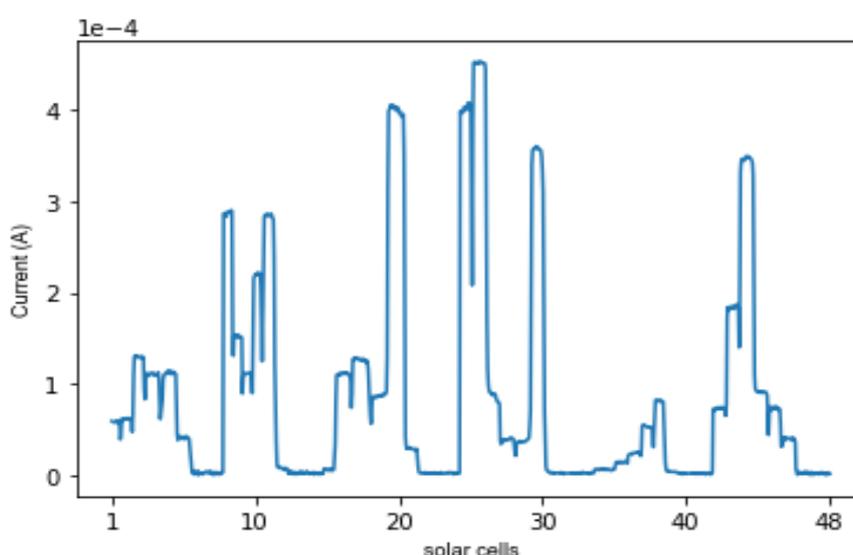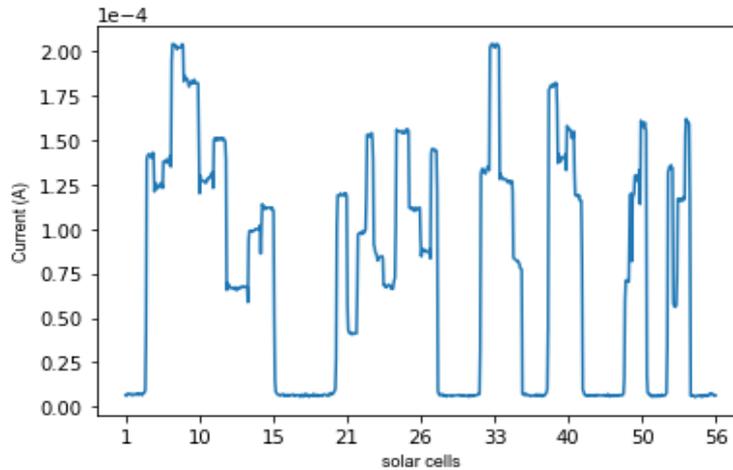

Fig. 7. Line scans for the c-Si module
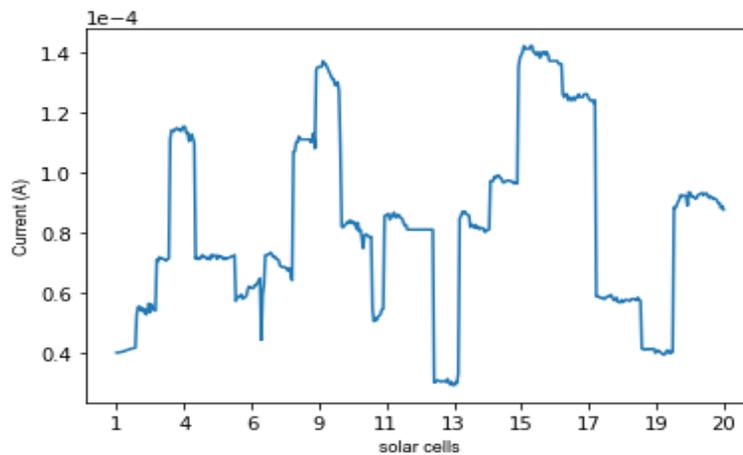
Fig. 8. Line scans for the mc-Si module

Fig. 9. Line scans for the a-Si module

Furthermore, even within the individual solar cell, there was non-uniformity in the current generated and this could have arisen from the non-uniform distribution of defects within the solar cell or from cracks developed during the soldering process (Kohler et al., 2014). The line scans were used to obtain the minimum and maximum photogenerated currents and to compute the percentage of performing solar cells in each PV module as indicated in Table 4.

From Table 3, the a-Si PV module had the highest percentage of performing solar cells among the three PV modules because only one of its solar cells had photogenerated currents near zero implying better overall performance. The mc-Si PV module had the lowest percentage of performing solar cells despite having the largest number of solar cells in the PV module, since most of them were nearly dead solar cells thus this module had some challenges in

Table 4. Comparative performance of three PV modules

PV type	Maximum I_{ph} (mA)	Minimum I_{ph} (μA)	Total number of solar cells in the module	Number of performing solar cells	Percentage of performing solar cells
c-Si	0.452	0.6	48	38	79
mc-Si	0.204	5.4	56	34	61
a-Si	0.142	29.5	20	19	95

maintaining optimal performance across its solar cells. The a-Si module also performed better because each of the solar cells had a larger cross-sectional area as compared to c-Si and mc-Si PV modules. In addition, a-Si had the lowest percentage of current mismatch at 79.2% as compared to c-Si and mc-Si with 99.9% and 97.4% respectively. In summary, the differences in the percentage of performing solar cells highlight variations in the performance and reliability of the three types of PV modules. The amorphous silicon module stands out with the highest percentage, indicating better overall performance.

3.2. Outdoor Characterization

The graphs for current against voltage (I-V curves) presented in Fig. 10 were obtained by plotting the average of five measurements taken at different intervals of the day. The I-V characteristics for each technology were then used in the determination of parameters like the V_{OC}, I_{sc}, V_{max}, I_{max} and P_{max} of the of the solar cells (Khunchan & Wiengmoon, 2018) as shown in Table 4.

The measured electrical performance parameters of the PV modules were compared with the manufacturers' rated specifications. Table 5 shows the comparison of the average measured and rated electrical solar parameters at a solar irradiance of 1000 Wm^{-2} for the three PV modules.

From Table 4, the measured maximum power and efficiencies for all three PV modules were below the rated values on the nameplates of the PV modules. This can be attributed to the poor performances of some of the individual solar cells in each of the PV modules as seen in the indoor line scan results. In addition, the c-Si, mc-Si, and a-Si modules had decrease in their marked power output of 1.5 W, 1.0 W and 1.1 W respectively. The decreases in the power output could be linked to the under performance of the individual solar cells in each of the PV modules. This implies that the identified poor performing solar cells had an impact on the performance of the PV module when it was fully installed for long-term operations. In addition, all the measured and rated efficiencies of the selected PV modules were below the industry-reported
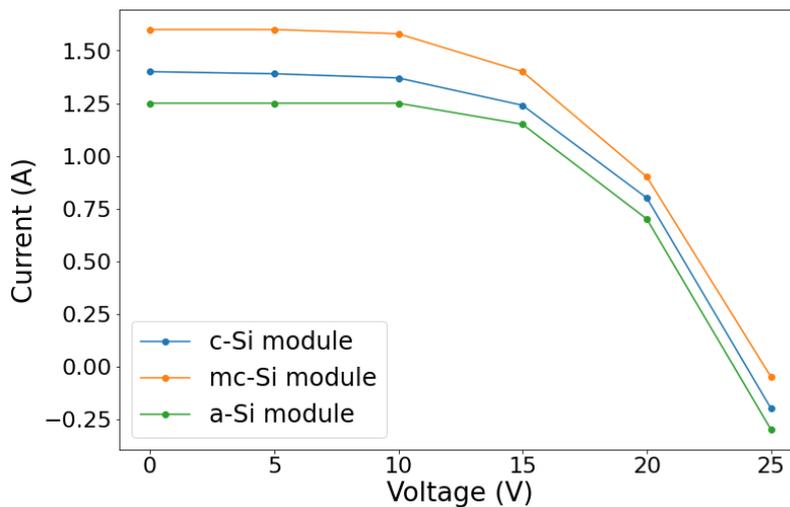

Fig. 10. I-V curves for the three different PV modules

Table 5. Comparison of the electrical parameters of three PV modules

Technology	Parameter	I_{sc}	V_{OC}	V_{max}	I_{max}	P_{max}	$\eta(\%)$
c-Si	Rated	1.27	21.4	17.4	1.15	20.0	16.2
	Measured	1.24	23.7	17.8	1.04	18.5	14.8
mc-Si	Rated	1.24	21.6	18.0	1.11	20.0	8.8
	Measured	1.55	24.4	17.3	1.10	19.0	8.4
a-Si	Rated	1.20	29.0	18.0	1.11	20.0	5.1
	Measured	1.27	23.8	17.8	1.06	18.9	4.8

efficiencies for c-Si, mc-Si, and a-Si of 24.4%, 20.4%, and 12.3% respectively (Green et al., 2021).

4. CONCLUSION

This research evaluated the performance of selected PV modules available in Ugandan markets using an indoor line scanning technique and an outdoor characterization method. The developed indoor line scanning quality control system generated line scans for each PV module, revealing that individual solar cells within a module performed differently. The percentage of performing solar cells in c-Si, mc-Si, and a-Si was 79%, 61%, and 95% respectively. In addition, from the outdoor characterization experimental results, the measured efficiencies for c-Si, mc-Si, and a-Si solar modules of 15.0%, 8.4%, and 4.8% that were lower than the rated values on the PV modules' nameplates. These findings indicate that the PV modules in the Ugandan market are underperforming in terms of efficiency and power output, aligning with public concerns about their poor performance. Therefore, before allowing imported PV modules to enter the Ugandan market, the government of Uganda through its competent authority (Uganda National Bureau of Standards) should consider implementing this proposed method or any other similar technology to evaluate the imported PV modules' performance. The study suggests government of Uganda to establish the PV testing system so that only well performing PV modules are allowed into the open market and this will help to build public confidence in the use of PV technology in Uganda.

DISCLAIMER (ARTIFICIAL INTELLIGENCE)

Author(s) hereby declare that NO generative AI technologies such as Large Language Models (ChatGPT, COPILOT, etc.) and text-to-image generators have been used during the writing or editing of this manuscript.

ACKNOWLEDGEMENT

COMPETING INTERESTS

Authors have declared that no competing interests exist.

REFERENCES

Aarakit, S. M., Ntayi, J. M., Wasswa, F., Adaramola, M. S., & Ssennono, V. F. (2021). Adoption of solar photovoltaic systems in households: Evidence from Uganda. *Journal of Cleaner Production, 329*, 129619.

Aarakit, S. M., Ssennono, V. F., & Adaramola, M. S. (2021). Estimating market potential for solar photovoltaic systems in Uganda. *Frontiers in Energy Research, 9*, 602468.

Aboagye, B., Gyamfi, S., Ofosu, E. A., & Djordjevic, S. (2022). Investigation into the impacts of design, installation, operation and maintenance issues on performance and degradation of installed solar photovoltaic (PV) systems. *Energy for Sustainable Development, 66*, 165–176.

Akinyele, D. O., Rayudu, R. K., & Nair, N.-K. C. (2015). Global progress in photovoltaic technologies and the scenario of development of solar panel plant and module performance estimation—Application in Nigeria. *Renewable and Sustainable Energy Reviews, 48*, 112–139.

Al-Dousari, A., Al-Nassar, W., Al-Hemoud, A., Alsaleh, A., Ramadan, A., Al-Dousari, N., & Ahmed, M. (2019). Solar and wind energy: Challenges and solutions in desert regions. *Energy, 176*, 184–194.

Alimi, O. A., Meyer, E. L., & Olayiwola, O. I. (2022). Solar photovoltaic modules' performance reliability and degradation analysis—a review. *Energies, 15*(16), 5964.

Alonso-Garcia, M. C., Ruiz, J. M., & Chenlo, F. (2006). Experimental study of mismatch and shading effects in the I–V characteristic of a photovoltaic module. *Solar Energy Materials and Solar Cells, 90*(3), 329–340.

Avellino, O. W. K., Mwarania, F., Wahab, A.-H. A., Aime, K. T., & Aime, K. T. (2018). Uganda solar energy utilization: Current status and future trends. *International Journal of Scientific and Research Publications (IJSRP), 8*(3), 317–327.

Badr, M. M., Hamad, M. S., Abdel-Khalik, A. S., Hamdy, R. A., Ahmed, S., & Hamdan, E. (2021). Fault identification of photovoltaic array based on machine learning

classifiers. *IEEE Access, 9*, 159113–159132.

Bakas, P., Marinopoulos, A., & Stridh, B. (2012). Impact of PV module mismatch on the PV array energy yield and comparison of module, string and central MPPT. *2012 38th IEEE Photovoltaic Specialists Conference*, 1393–1398.

Blonquist Jr, J. M., & Bugbee, B. (2020). Solar, net, and photosynthetic radiation. *Agroclimatology: Linking Agriculture to Climate, 60*, 1–49.

Cáceres, M., Firman, A., Montes-Romero, J., González Mayans, A. R., Vera, L. H., Fernández, E. F., & de la Casa Higueras, J. (2020). Low-cost I–V tracer for PV modules under real operating conditions. *Energies, 13*(17), 4320.

Celik, I., Philips, A. B., Song, Z., Yan, Y., Ellingson, R. J., Heben, M. J., & Apul, D. (2017). Energy payback time (EPBT) and energy return on energy invested (EROI) of perovskite tandem photovoltaic solar cells. *IEEE Journal of Photovoltaics, 8*(1), 305–309.

Chamberlin, C. E., Lehman, P., Zoellick, J., & Pauletto, G. (1995). Effects of mismatch losses in photovoltaic arrays. *Solar Energy, 54*(3), 165–171.

Chantana, J., Horio, Y., Kawano, Y., Hishikawa, Y., & Minemoto, T. (2019). Spectral mismatch correction factor for precise outdoor performance evaluation and description of performance degradation of different-type photovoltaic modules. *Solar Energy, 181*, 169–177.

Crozier, J. L., Van Dyk, E. E., & Vorster, F. J. (2012). Characterization of cell mismatch in a multi-crystalline silicon photovoltaic module. *Physica B: Condensed Matter, 407*(10), 1578–1581.

Crozier, J. L., van Dyk, E. E., & Vorster, F. J. (2015). Identification and characterisation of performance limiting defects and cell mismatch in photovoltaic modules. *Journal of Energy in Southern Africa, 26*(3), 19–26.

da Fonseca, J. E. F., de Oliveira, F. S., Prieb, C. W. M., & Krenzinger, A. (2020). Degradation analysis of a photovoltaic generator after operating for 15 years in southern Brazil. *Solar Energy, 196*, 196–206.

De la Parra, I., Muñoz, M., Lorenzo, E., García, M., Marcos, J., & Martínez-Moreno, F. (2017). PV performance modelling: A review in the light of quality assurance for

large PV plants. *Renewable and Sustainable Energy Reviews, 78*, 780–797.

Devi, H. R., Bisen, O. Y., Nanda, S., Nandan, R., & Nanda, K. K. (2021). Internal versus external quantum efficiency of luminescent materials, photovoltaic cells, photodetectors and photoelectrocatalysis. *Current Science, 894–898.*

Duke, R. D., Jacobson, A., & Kammen, D. M. (2002). Photovoltaic module quality in the Kenyan solar home systems market. *Energy Policy, 30*(6), 477–499.

Electricity Regulatory Authority. (2024, September 28). Installed Capacity. Webpage. https://www.era.go.ug/index.php/stats/generation-statistics/installed-capacity

Fashina, A., Mundu, M., Akiyode, O., Abdullah, L., Sanni, D., & Ounyesiga, L. (2018). The drivers and barriers of renewable energy applications and development in Uganda: A review. *Clean Technologies, 1*(1), 9–39.

Gebreslassie, M. G. (2021). Development and manufacturing of solar and wind energy technologies in Ethiopia: Challenges and policy implications. *Renewable Energy, 168*, 107–118.

Green, M., Dunlop, E., Hohl-Ebinger, J., Yoshita, M., Kopidakis, N., & Hao, X. (2021). Solar cell efficiency tables (version 57). *Progress in Photovoltaics: Research and Applications, 29*(1), 3–15.

Hasan, K., Yousuf, S. B., Tushar, M. S. H. K., Das, B. K., Das, P., & Islam, M. S. (2022). Effects of different environmental and operational factors on the PV performance: A comprehensive review. *Energy Science & Engineering, 10*(2), 656–675.

Hejri, M., & Mokhtari, H. (2016). On the comprehensive parametrization of the photovoltaic (PV) cells and modules. *IEEE Journal of Photovoltaics, 7*(1), 250–258.

Huld, T., Gottschalg, R., Beyer, H. G., & Topič, M. (2010). Mapping the performance of PV modules, effects of module type and data averaging. *Solar Energy, 84*(2), 324–338.

Ibrahim, H., & Anani, N. (2017). Variations of PV module parameters with irradiance and temperature. *Energy Procedia, 134*, 276–285.

Islam, M. A., Hasanuzzaman, M., & Abd Rahim, N. (2018). Investigation of the potential induced degradation of on-site aged polycrystalline PV modules operating in Malaysia. *Measurement, 119*, 283–294.

Kaspari, C., Zorn, M., Weyers, M., & Erbert, G. (2008). Growth parameter optimization of

the GaInP/AlGaInP active zone of 635 nm red laser diodes. *Journal of Crystal Growth, 310*(23), 5175–5177.

Kaushika, N. D., & Rai, A. K. (2007). An investigation of mismatch losses in solar photovoltaic cell networks. *Energy, 32*(5), 755–759.

Kazem, H. A., & Chaichan, M. T. (2015). Effect of humidity on photovoltaic performance based on experimental study. *International Journal of Applied Engineering Research (IJAER), 10*(23), 43572–43577.

Khunchan, S., & Wiengmoon, B. (2018). Method to determine the single curve IV characteristic parameter of solar cell. *Journal of Physics: Conference Series, 1144*(1), 12012.

Kohler, D., Zuschlag, A., & Hahn, G. (2014). On the origin and formation of large defect clusters in multicrystalline silicon solar cells. *Solar Energy Materials and Solar Cells, 120*, 275–281.

Kumar, M., & Kumar, A. (2019). Experimental validation of performance and degradation study of canal-top photovoltaic system. *Applied Energy, 243*, 102–118.

Kumar, S., Alheloo, A., Hassan, S., Hanifi, H., Alhamadani, H., Alshanqiti, H., John, J. J., Mathiak, G., & Alberts, V. (2021). Investigation and analysis of defects and degradations in desert fielded photovoltaic modules. *2021 IEEE 48th Photovoltaic Specialists Conference (PVSC)*, 788–792.

Lee, H.-C., & Chang, C.-T. (2018). Comparative analysis of MCDM methods for ranking renewable energy sources in Taiwan. *Renewable and Sustainable Energy Reviews, 92*, 883–896.

Li, B., Diallo, D., Migan-Dubois, A., & Delpha, C. (2023). Performance evaluation of IEC 60891: 2021 procedures for correcting I–V curves of photovoltaic modules under healthy and faulty conditions. *Progress In Photovoltaics: Research And Applications, 31*(5), 474–493.

Luo, W., Clement, C. E., Khoo, Y. S., Wang, Y., Khaing, A. M., Reindl, T., Kumar, A., & Pravettoni, M. (2021). Photovoltaic module failures after 10 years of operation in the tropics. *Renewable Energy, 177*, 327–335.

Micheal, M., Yu, H., Cheng, S., Yrausquin, E. P., & Arnaud, K. L. (2018). Uganda's energy security based on prospects, challenges, opportunities, supply, and demand towards achieving a green energy-reliant environment. *International Journal of Energy Engineering, 8*(2), 40–51.

Mugagga, R. G., Chamdimba, H. B. N., & Chamdimba, N. (2019). A comprehensive review on the status of solar PV growth in Uganda. *Journal of Energy Research and Reviews, 3*(4), 1–14.

Nnamchi, S. N., Nnamchi, O. A., Nwaigwe, K. N., Jagun, Z. O., & Ezenwankwo, J. U. (2021). Effect of technological mismatch on photovoltaic array: Analysis of relative power loss. *Journal of Renewable Energy and Environment, 8*(4), 77–89.

Okello, D., Mubiru, J., & Banda, E. J. K. (2011). Availability of direct solar radiation in Uganda. *30th ISES Biennial Solar World Congress*, 3554–3563.

Padilla, A., Londoño, C., Jaramillo, F., Tovar, I., Cano, J. B., & Velilla, E. (2022). Photovoltaic performance assessment by correcting the IV curves in outdoor tests. *Solar Energy, 237*, 11–18.

Quansah, D. A., Adaramola, M. S., Takyi, G., & Edwin, I. A. (2017). Reliability and degradation of solar PV modules—case study of 19-year-old polycrystalline modules in Ghana. *Technologies, 5*(2), 22.

Rabelo, M., Park, H., Kim, Y., Cho, E.-C., & Yi, J. (2021). Corrosion, LID, and LeTID in silicon PV modules and solution methods to improve reliability. *Transactions on Electrical and Electronic Materials, 22*(5), 575–583.

Santhakumari, M., & Sagar, N. (2019). A review of the environmental factors degrading the performance of silicon wafer-based photovoltaic modules: Failure detection methods and essential mitigation techniques. *Renewable and Sustainable Energy Reviews, 110*, 83–100.

Shenouda, R., Abd-Elhady, M. S., & Kandil, H. A. (2022). A review of dust accumulation on PV panels in the MENA and the Far East regions. *Journal of Engineering and Applied Science, 69*(1), 8.

Singh, R., Sharma, M., & Yadav, K. (2022). Degradation and reliability analysis of photovoltaic modules after operating for 12 years: A case study with comparisons. *Renewable Energy, 196*, 1170–1186.

Sun, X., Chung, H., Chavali, R. V. K., Bermel, P., & Alam, M. A. (2017). Real-Time Monitoring of Photovoltaic Reliability Only Using Maximum Power Point—The Suns-Vmp Method. *2017 IEEE 44th Photovoltaic Specialist Conference (PVSC)*, 1904–1907.

Tahir, Z. R., Kanwal, A., Asim, M., Bilal, M., Abdullah, M., Saleem, S., Mujtaba, M. A.,

Veza, I., Mousa, M., & Kalam, M. A. (2022). Effect of temperature and wind speed on efficiency of five photovoltaic module technologies for different climatic zones. *Sustainability, 14*(23), 15810.

Takyi, G. (2017). Correlation of infrared thermal imaging results with visual inspection and current-voltage data of PV modules installed in Kumasi, a hot, humid region of sub-Saharan Africa. *Technologies, 5*(4), 67.

Touati, F. A., Al-Hitmi, M. A., & Bouchech, H. J. (2013). Study of the effects of dust, relative humidity, and temperature on solar PV performance in Doha: Comparison between monocrystalline and amorphous PVs. *International Journal of Green Energy, 10*(7), 680–689.

Tyagi, V. V., Rahim, N. A. A., Rahim, N. A., Jeyraj, A., & Selvaraj, L. (2013). Progress in solar PV technology: Research and achievement. *Renewable and Sustainable Energy Reviews, 20*, 443–461.

van Hove, E., & Johnson, N. G. (2021). Refugee settlements in transition: Energy access and development challenges in Northern Uganda. *Energy Research & Social Science, 78*, 102103.

Wurster, T. S., & Schubert, M. B. (2014). Mismatch loss in photovoltaic systems. *Solar Energy, 105*, 505–511.

Yunus Khan, T. M., Soudagar, M. E. M., Kanchan, M., Afzal, A., Banapurmath, N. R., Akram, N., Mane, S. D., & Shahapurkar, K. (2020). Optimum location and influence of tilt angle on performance of solar PV panels. *Journal of Thermal Analysis and Calorimetry, 141*, 511–532.

Zefri, Y., ElKettani, A., Sebari, I., & Ait Lamallam, S. (2018). Thermal infrared and visual inspection of photovoltaic installations by UAV photogrammetry—Application case: Morocco. *Drones, 2*(4), 41.

Zhang, T., Shi, X., Zhang, D., & Xiao, J. (2019). Socio-economic development and electricity access in developing economies: A long-run model averaging approach. *Energy Policy, 132*, 223–231.

Peer-review history:
The peer review history for this paper can be accessed here:
https://www.sdiarticle5.com/review-history/126855